NANOSYSTEMS: PHYSICS, CHEMISTRY, MATHEMATICS, 2014, 5 (6), P. 811–819

MEASURING LOCAL QUANTUM YIELD OF PHOTOLUMINESCENCE AND PHOTOTRANSFORMATIONS WITH LASER SCANNING MICROSCOPE

V. V. Zakharov[1,2], M. A. Baranov[1], A. S. Zlatov[1], A. V. Veniaminov[1]

[1]ITMO University, St. Petersburg, Russia
[2]Optec LLC, St. Petersburg, Russia

Viktor-zah@yandex.ru, mbaranov@mail.ru, zlatov.andrei@gmail.com, veniaminov@phoi.ifmo.ru

PACS 78.55.Qr, 82.50.-m, 68.37.-d, 82.30.Qt

Measurement of local quantum yields for the photoluminescence of semiconductor nanocrystals (quantum dots) and photoinduced transformations of dye molecules in polymer films is demonstrated using a laser scanning microscope capable of mapping luminescence spectra and intensities of transmitted laser light. The confocal scanning microscope (Zeiss LSM710) was applied for both the induction of photochemical transformations and measurement The luminescence quantum yield values for quantum dots in different locations of a polymer film were found to differ, ostensibly depending on their aggregation. To measure photoisomerization quantum yield, the effects of scanning a tiny area of a polymer film with a focused beam on the intensities of luminescence and transmitted light were monitored.

Keywords: Confocal microscopy, luminescence, photoisomerization, quantum dot, thioindigo.

Received: 24 November 2014
Revised: 29 November 2014

1. Introduction

Quantum yield (QY) is one of the most important characteristics of photoinduced processes such as photoluminescence and photochemical transformations. The quantum yield depends on intrinsic properties of molecules, nanocrystals, and other species as well as on their interactions with the environment. As a rule, only values for QY averaged over relatively large areas can be measured, while information about their microscopic local values remains hidden.

Nanocomposites with luminescent semiconductor nanocrystals (quantum dots, QD) are widely used in different areas, such as microelectronics, solar energy conversion, biology and medicine [1, 2] due to their unusual optical, electrical and structural properties [3]. Spatial heterogeneity of properties is a common feature of nanocomposite materials. Aggregation of nanoparticles may lead to considerable inhomogeneity of light intensity, decrease of luminescence caused by nonradiative energy transfer. The distribution of the QY could be regarded as a quantitative measure of nanocrystal and molecular interactions and provide information about efficiency of nanocrystal incorporation in the polymeric matrix. Bulk polymers are known to be spatially inhomogeneous, and luminescent dyes dissolved in them may serve efficient probes for testing microheterogeneous environment, provided local QY becomes available.

There are two different approaches to measuring QY of luminescence: (i) direct, or absolute, which typically requires a spectrophotometer with an integrating sphere, and (ii) comparative, based on relative measurements of light emitted by a specimen under study and

a fluorescent standard with known QY. Traditional techniques of QY measurements, as well as possible sources of errors, have been analyzed and described in detail [4–9]. In a similar way, the QY of photochemical reactions can be obtained from spectroscopic monitoring of photoreaction progress and comparison with phototransformations of etalon substances whose QY are well established (chemical actinometers) [10] or by direct measurement of exposure.

Various techniques intended for the measurement of absolute luminescence and photoreaction QY are known, such as that using a spectrophotometer with integrating sphere [11] or the dual-beam thermal lens technique [12], but only in a few publications local characteristics with microscopic resolution have been revealed. Thus, a combined map of topography and single-particle fluorescence QY of single particles was obtained using correlated atomic-force and single-particle fluorescence microscopy [13], however such a technique could hardly be applied to investigate the inhomogeneous bulk of thick samples.

The present work is aimed at the development of a technique utilizing a confocal laser scanning microscope (LSM) for the measurement of local QY of exemplary photoprocesses induced by laser light in doped polymer films: quantum dot luminescence and phototransformations of organic molecules such as *trans-cis* photoisomerization of a thioindigo derivative and photoreduction of phenanthrenequinone.

2. Experimental

2.1. Instrumentation and calibration

In this study, a Zeiss LSM710 scanning microscope based on Axio Imager Z1 stand, Carl Zeiss Microimaging GmbH, Germany, was used to measure QY. Confocal scanning microscopy allows one to obtain digital images with high spatial resolution due to the filtering-out of light scattered and emitted by out-of-focus optical slices. The LSM is capable of measuring the intensity of laser light transmitted by specimens and obtaining local luminescence spectra.

Prior to applying the microscope for numerical measurements of QY, we needed to assess the accuracy of light transmittance measured with its help and calibrate the spectral response of the microscope photodetector system, in order to ensure correct calculation of photons absorbed by the species and inducing their luminescence or phototransformations.

To verify the accuracy of quantitative measurements using LSM, the transmittance of laser light by several neutral gray light absorbers (glass plates with thin metal coating of controlled thickness) with well defined optical densities was measured. The measured optical densities versus their etalon values are presented in Fig. 1 that demonstrates perfect agreement within the range of optical densities up to 1 and slight deviation at O.D.=2.4, for the small aperture (0.2) lens. In the case of large numerical aperture (0.95), a significant deviation from linearity shall be taken into account already for O.D.$>$0.6, which is already far beyond absorbance values considered acceptable for luminescence measurements.

For the present study, objective lenses were chosen with sufficiently small numerical aperture (predominantly 0.1 to 0.2) that ensured, along with correct transmittance measurements, ‘optical slice thickness’ larger than the sample thickness, to avoid possible uncertainties caused by absorption heterogeneity along the optical axis. Axial resolution of luminescence images strongly depends not only on numerical aperture, but also on the diameter of the confocal pinhole (Fig. 2); however, this does not apply to transmittance measurements that do not involve the pinhole.

Spectral calibration of LSM photodetector system was performed using an etalon incandescent lamp verified at S. I. Vavilov Optical institute (St. Petersburg) as black body with color

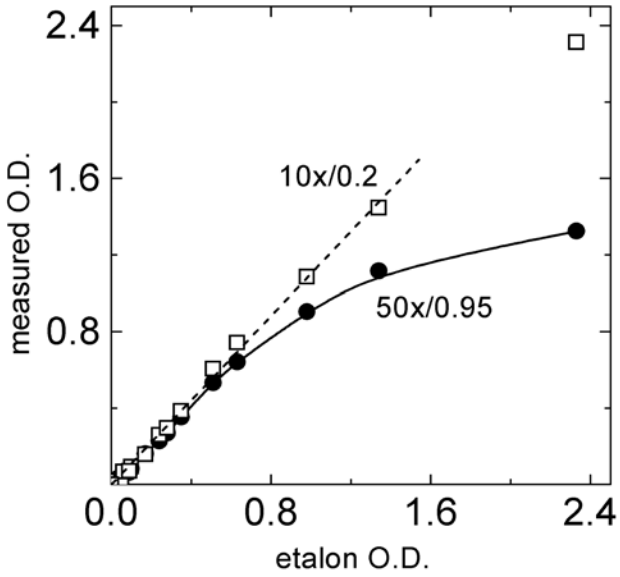

FIG. 1. Optical density of neutral gray etalon absorbers at 543 nm measured with LSM using two different objective lenses (magnification / numerical aperture: $10 \times /0.2$, squares and $50 \times /0.95$, circles), vs. nominal etalon optical density. The dashed line is the best linear fit for the low aperture dependence; the solid curve is exponential fit for the large aperture drawn as a guide to the eye

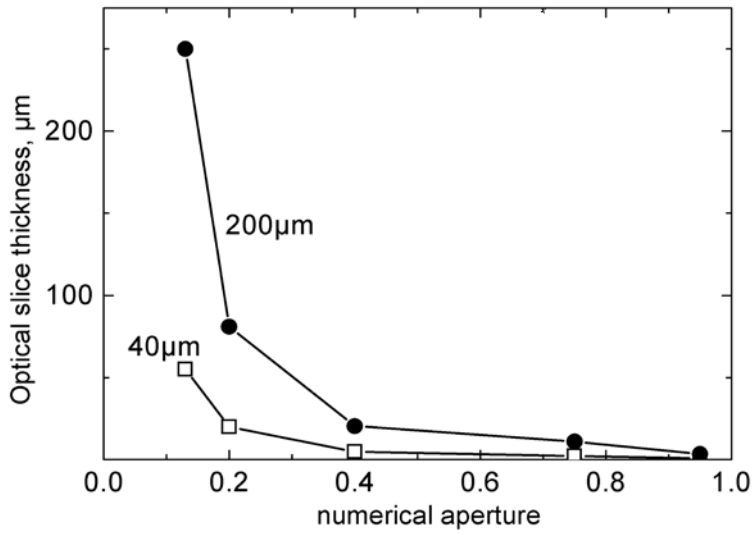

FIG. 2. Optical slice thickness as a function of numerical apertures of the objective lenses, at confocal pinhole diameters 40 (squares) and 200 μm (circles)

temperature $T = 2856$ K; the spectra of its emission measured with the LSM was used for correction of the luminescence spectra.

Diode (405 nm), Ar^+ (488 nm) and He–Ne (543 nm) lasers served as light sources for luminescence excitation and the induction of phototransformations. In order to avoid overheating of specimens by focused laser beams, not more than a few per cent of maximum power was used in the measurements. Within these limits, no effect of varied power on the results of measurements was revealed.

The temperature of specimens could be monitored and stabilized during the measurements within the range from room temperature up to 100 °C with an accuracy of ± 0.125 °C using a glass substrate with conductive coating serving as a heater run by a specially designed LabView-compatible controller. Almost all the measurements were fulfilled at 24 °C.

2.2. Sample preparation

The polymer films were made by casting from tetrahydrofuran solutions of polymers: polybutylmethacrylate (PBMA), polymethylmethacrylate (PMMA), polyvinylbutyral, or polycarbonate mixed in appropriate proportions with solutions of either semiconductor quantum dots (QD), thioindigo dye (TI), phenanthrenequinone (PQ), or Rhodamine 6G (R6G) onto polished glass plates. The polymer powders were purchased from Vekton (St. Petersburg, Russia).

The photoisomerizing thioindigo derivative [14] was synthesized and kindly presented by Dr. M. Mostoslavsky and Dr. V. Paramonov (NIOPIK branch, Rubezhnoe, Ukraine) and remained in the possession of our laboratory. Previously, this compound served in 3D holography as a photoswitchable sensitizer of anthracene photooxidation in Reoxan media that helped convert weak amplitude 'latent image' into efficient phase holograms [15]. The dye was used in the present work after its absorption and luminescence spectra were found to remain unchanged.

Phenanthrenequinone (PQ), which was purchased from Aldrich, is capable of photoreduction through hydrogen abstraction from surrounding molecules [16] and is known as a key component of light-sensitive materials with postexposure development of holograms by photoattachment and molecular diffusion [17].

Core/shell CdSe/ZnS QDs, with average diameter of 2.5 nm and capped by trioctylphosphineoxide (TOPO), were synthesized and tested in Belarusian State University, Minsk, Belarus. For hexane solutions of the QDs, the maximum luminescence was found at 531 nm, with QY of ~ 13 %.

3. Results and Discussion

3.1. Luminescence of quantum dots

Luminescence quantum yield of QDs in a polycarbonate film was determined by a comparative technique using a similar film with R6G as an intermediate fluorescence reference, whose QY (47 %) was previously determined in turn by comparison with R6G solution in ethanol (QY= 94 %):

$$\phi = \phi_R \frac{I}{I_R} \frac{OD_R}{OD} \frac{n^2}{n_R^2}, \tag{1}$$

where ϕ is QY, I is luminescence intensity integrated over the whole spectrum, n is refractive index, OD is optical density and the subscript R stands for reference.

While no spatial inhomogeneity was found in R6G luminescence intensity, the luminescent image of polycarbonate film with QDs (Fig. 3a) manifests their uneven spatial distribution, with apparently uniformly luminescent area with dark holes in the left part and small bright spots on the right. Quantum yields of QD luminescence in these areas were found to differ: 0.4 in the uniform layer and 0.12 in the agglomerates (circle), despite the apparently brighter luminescence in the latter case. The lower QY value within the rounded spot in Fig. 3a can be explained by stronger interaction between agglomerated QDs as compared to less densely distributed QDs in the rectangular area, which also correlates with notably larger red shift of the luminescence spectrum (Fig. 3b) in the latter case with respect to QD luminescence spectrum in liquid (hexane) solution (531 nm). It should be noted that, contrastingly, QD luminescence in a

polyvinylbutyral film was found to be uniform, with QY = 0.23 and maximum luminescence at 534 nm.

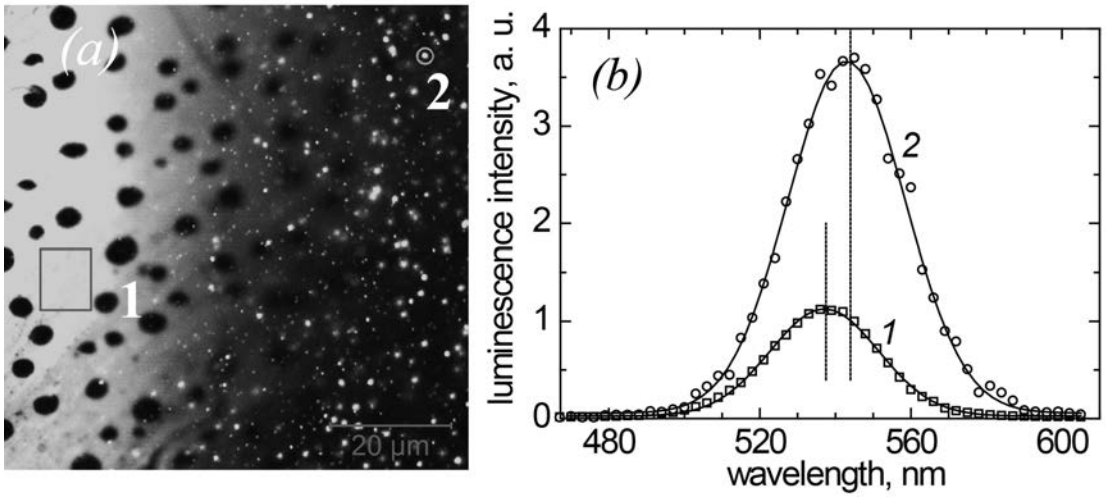

FIG. 3. a) Luminescent image of a 80×80 μm part of a polycarbonate film with CdSe/ZnS nanocrystals; excitation wavelength 405 nm; b) luminescence spectra of the film region within the rectangle 1 and the bright spot in the centre of the circle 2 (squares and circles, respectively). Solid lines are best Gaussian fits; dotted lines depict the maxima of luminescence intensity at 537 (1) and 543 nm (2). Notice the lower intensity in the area 1 with QY larger than that in the area 2

3.2. Photoisomerization of thioindigo dye

The thioindigo dye exists in two isomeric forms that can undergo reversible phototransformations accompanied by dramatic spectral changes. In Fig. 4, absorption spectra of the TI-doped PBMA film obtained after exposures to mercury arc light with wavelengths 578 nm (curve *1*) and 436 nm (*2*) are plotted, representing almost pure *trans*-isomer and isomer mixture with predominant contribution of *cis*-isomer, respectively. Only *trans*-TI molecules are capable of fluorescence [14, 18] whose intensity can be then a measure of their concentration. Almost identical fluorescence spectra acquired with LSM and Cary Eclipse spectrofluorimeter are also presented in Fig. 4 (*3* and *4*, respectively).

To study *trans-cis*-photoisomerization of TI, different exposures of actinic light were applied to small strip-shaped areas of the specimen by scanning them with a He-Ne laser (543 nm) of the microscope, followed by monitoring transmittance and luminescence excited by properly attenuated light of the same laser. The intensities of emitted and transmitted light are shown in Fig. 5 as functions of exposure. Before the measurements, the dye in the film was brought into the *trans*-isomeric form by uniform exposure to 436 nm light of a 120 W high-pressure mercury lamp.

Unlike fluorescence, light absorbance at the excitation wavelength does not exclusively belong to *trans*-isomer. Therefore, the optical density of the film at 543 nm can be taken as a measure of *trans*-isomer concentration only at low degree of *trans-cis* conversion, in the initial stage of the process. Hence, we consider luminescence intensity more reliable for monitoring the dynamics of phototransformation, while the initial value of optical density was used to determine the number of TI molecules.

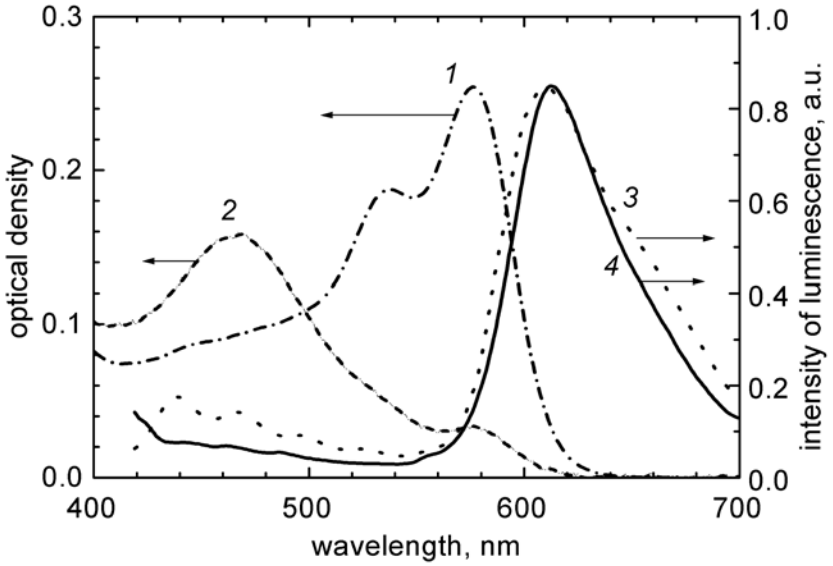

FIG. 4. Absorption spectra of polymer film with thioindigo dye exposed to light with wavelength 436 nm (*1*, dash-dotted line, almost pure *trans*-isomer) and 578 nm (*2*, dashed line, predominantly *cis*-isomer with small contribution of *trans*-isomer); fluorescence spectra measured with LSM (*3*, dotted line) and Cary Eclipse spectrofluorimeter (*4*, solid line; excitation at 405 nm)

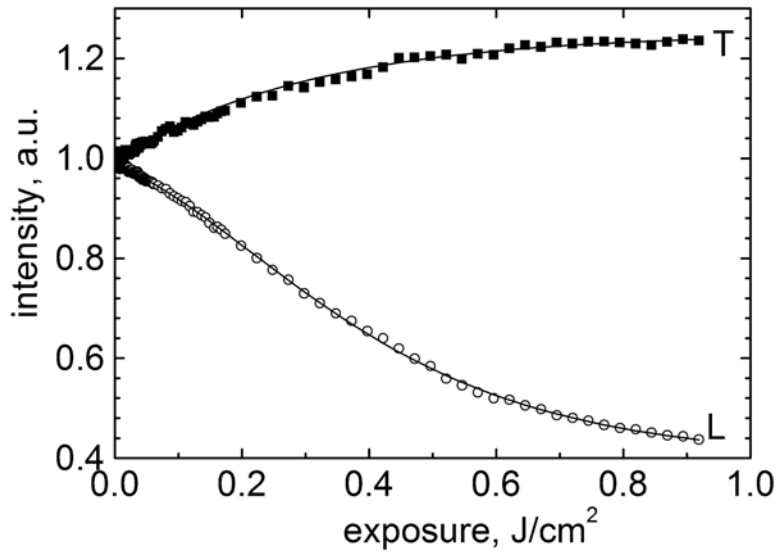

FIG. 5. Photoisomerization of thioindigo in PBMA film monitored with LSM: intensities of transmitted excitation light (543 nm, solid line, T) and luminescence of the *trans*-isomer (dashed line, L) as functions of exposure

The QY of the *trans-cis* photoisomerization can be calculated as ratio of the number $\Delta D N_A S/\alpha$ of molecules within the illuminated area S converted from *trans*- to *cis*-isomer divided by the number $E\,(1-T)\,/h\nu$ of absorbed photons with energy $h\nu$:

$$\phi_{tc} = \frac{\Delta D S N_A h\nu}{E\alpha\,(1-T)}, \tag{2}$$

with ΔD- the small photoinduced change of optical density caused by exposure to light energy E, N_A – Avogadro number, $a = 8700$ Lmol^{-1}·cm^{-1} – molar absorption coefficient of *trans*-TI calculated using the spectroscopic data available from [14], T – transmittance of the doped film at 543 nm.

The initial (measured when almost all the dye was in *trans*-isomeric form) value of ϕ_{tc}= 0.006 is between the values previously reported for QY of *trans-cis* isomerization of TI in more rigid PMMA and in liquid butyl acetate solution, 0.001 and 0.06, respectively [19]. During photoisomerization, ϕ_{tc} dramatically decreased after about 30 – 35 % of *trans*-molecules had been converted to the *cis*-isomer (Fig. 6). This was presumably due to the significantly heterogeneous distribution of free volume needed for restructuring dye molecules in the bulk polymer, even though glass transition temperature of PBMA is quite close to the measurement temperature. Contrastingly, QY of fluorescence that apparently does not require much free volume did not significantly vary from its initial value (0.15).

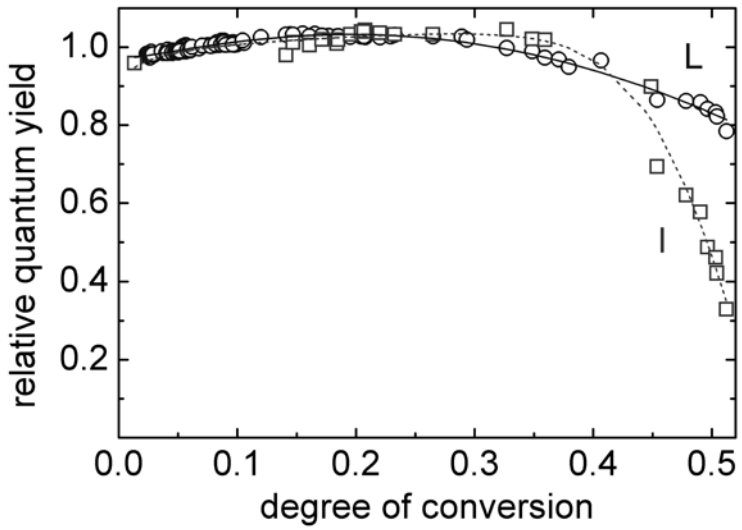

FIG. 6. Quantum yields of isomerization (squares, I) and luminescence (circles, L) as functions of degree of dye conversion from *trans*- to *cis*-isomeric form in the course of isomerization. Lines are guides to the eye

3.3. Photoreduction of phenanthrenequinone

Photoreduction of PQ provided another example of a photochemical process for this study. Different doses of laser light (488 nm) were applied to 50×50 μm squares of PQ-doped PMMA film using the scanning microscope (Fig. 7a). As a result of the exposure, PQ was partially bleached and the film transmittance has grown, as well as its luminescence intensity (Fig. 7b) – the situation contrary to that of photoisomerization (cf. Figs. 5 and 8). This means that the luminescence belongs to the photoproduct, despite the latter is known to have almost negligible absorption in the visible range. Because absorbance of the photoproduct at the wavelength of excitation remained unknown, no QY of its luminescence could be calculated.

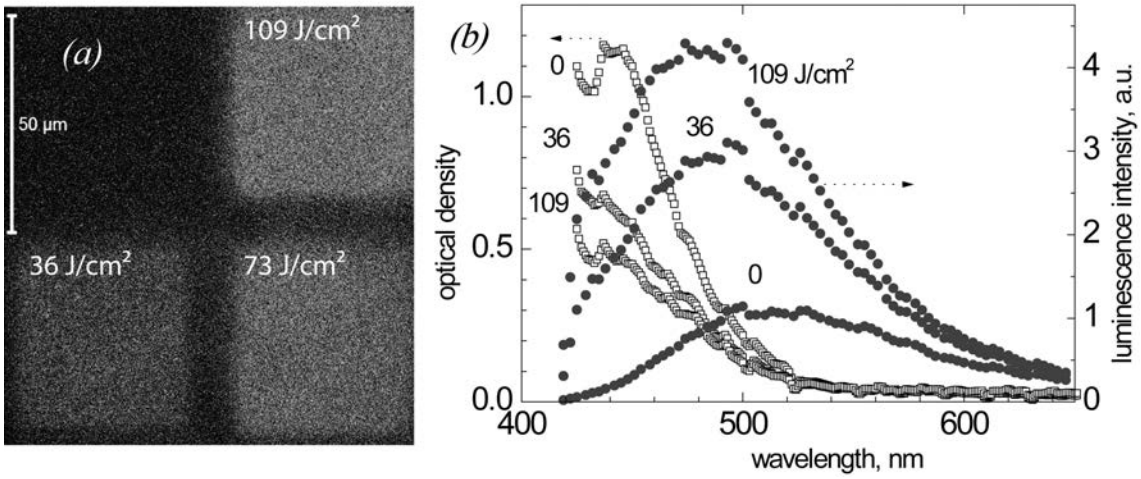

FIG. 7. Phototransformation of phenanthrenequinone in PMMA: a) luminescent image of a 100×100 μm^2 part of a PMMA film with PQ; the lighter square areas were exposed to 36, 73 and 109 J/cm^2 of laser light at 488 nm before scanning for imaging; (b) local optical density (open symbols) and luminescence spectra (full symbols) of the film in its intact state (0) and after 36 and 109 J/cm^2 exposure at 488 nm

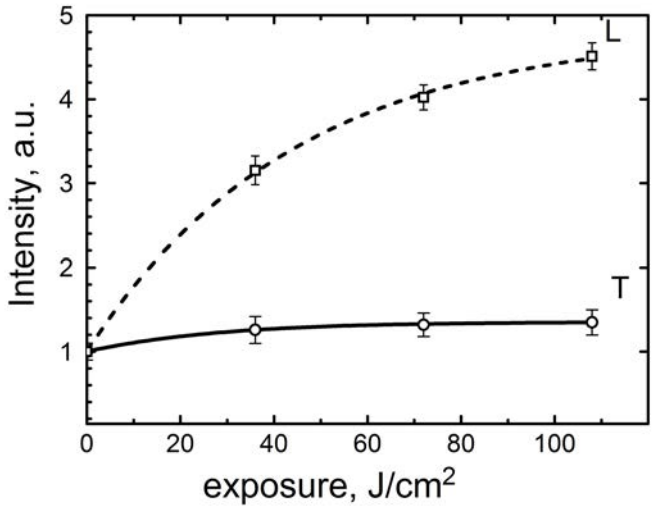

FIG. 8. Relative intensities of transmitted light (T, 488 nm) and luminescence of the film at 500 nm (L, excitation wavelength 405 nm) measured with LSM, as functions of exposure

The QY of PQ phototransformation was calculated similar to that of photoisomerization and was approximately 10 percent.

4. Conclusions

In this study, we gave three examples of using a confocal scanning microscope as a convenient tool for measuring local quantum yields of luminescence and photochemical transformations. This application of the precision imaging instrumentation is based on its ability to measure the spatial distributions and the intensities of sample-related transmitted and emitted

light, obtain local luminescence spectra, and expose small regions of interest to photochemically active light. Such measurements can provide important information on microstructure of composite materials, their spatial heterogeneity, and can also be helpful if only a small amount or small area of a specimen is available for study.

Acknowledgments

The authors gratefully acknowledge the financial support of this work from the Ministry of Education and Science of the Russian Federation (Grant No. 14.B25.31.0002) and the Russian Foundation for Basic Research (Grants No. 12-02-01263 and No. 12-02-00938).

References

[1] Rajeshwar K., de Tacconi N.R., Chenthamarakshan C.R. Semiconductor-Based Composite Materials: Preparation, Properties, and Performance. *Chem. Mater.*, **13**, P. 2765–2782 (2001).

[2] Tomczak N., Janyczewski D., Han M., Vancso G.J. Designer polymer-quantum dot architectures. *Progr. Polymer Sci.*, **34**, P. 393–430 (2009).

[3] Bukowski T.J., Simmons J.H. Quantum Dot Research: Current State and Future Prospects. *Critical Reviews in Solid State and Materials Sciences*, P. 119–142 (2002).

[4] Demas J.N., Crosby G.A. The Measurement of Photoluminescence Quantum Yields. *Review, J. Phys. Chem.*, **75**, P. 991–1024 (1971).

[5] Williams A.T.R., Winfield S.A., Miller J.N. Relative fluorescence quantum yields using a computer controlled luminescence spectrometer. *Analyst*, **108**, P. 1067–1071 (1983).

[6] Lakowicz J.R. *Principles of Fluorescence Spectroscopy*, 3rd ed. Springer, 954 p. (2006).

[7] Carlson L., Krauss T.D. Direct measurement of the fluorescence quantum yield for individual single-walled carbon nanotubes. *Proc. Conf. Electrochem. Soc. 'Carbon Nanotubes and Nanostructures: Fundamental Properties and Processes'*, Abstr. 1018 (2007).

[8] Brouwer A.M. Standards for photoluminescence quantum yield measurements in solution (IUPAC Technical Report). *Pure Appl. Chem.*, **83**, P. 2213–2228 (2011).

[9] Wuerth C., Grabolle M., et al. Relative and absolute determination of fluorescence quantum yields of transparent samples. *Nature Protocols*, **8**, P. 1535–1550 (2013).

[10] Kuhn H.J., Braslavsky S.E., Schmidt R. Chemical Actinometry (IUPAC Technical Report). *Pure Appl. Chem.*, **76**, P. 2105–2146 (2004).

[11] Gaigalas A.K., Wang L. Measurement of the fluorescence quantum yield using a spectrometer with an integrating sphere detector. J. *Res. Natl. Inst. Stand. Technol.*, **113**, P. 17–28 (2008).

[12] Bindhu C.V., Harilal S.S., et al. Measurement of the absolute fluorescence quantum yield of rhodamine B solution using a dual-beam thermal lens technique. *J. Phys. D: Appl. Phys.*, **29**, P. 1074–1079 (1996).

[13] Ebenstein Y., Mokari T., Banina U. Fluorescence quantum yield of CdSe/ZnS nanocrystals investigated by correlated atomic-force and single-particle fluorescence microscopy. *Appl. Phys. Lett.*, **80**, P. 4033 (2002).

[14] Mostoslavskii M.A. Photochromic Thioindigoid Dyes. In: Organic Photochromes, ed. by Eltsov A.V., Springer, New York and London, P. 45–104 (1990).

[15] Lashkov G.I., Popov A.P., Ratner O.B. Three-dimensional phase-recording reoxan media with physical development of a latent image. *Opt. Spectrosc.*, **52**, P. 350–352 (1982).

[16] P.A. Carapellucci, H.P. Wolf, K. Weiss. Photoreduction of 9,10-Phenanthrenequinone. *J. Amer. Chem. Soc.*, **91**, P. 4635–4639 (1969).

[17] Veniaminov A.V., Mahilny U.V. Holographic Polymer Materials with Diffusion Development: Principles, Arrangement, Investigation, and Applications. *Opt. Spectrosc.*, **115**, P. 902–925 (2013).

[18] Haucke G., Paetzold R. *Photophysikalische Chemie Indigoider Farbstoffe. Nova Acta Leopoldina*. Deutsche Akademie der Naturforscher Leopoldina, Halle (Saale), 123 p. (1978).

[19] Veniaminov A.V., Lashkov G.I. Photochemical isomerization of thioindigo derivatives embedded in poly(methylmethacrylate). *Polymer Sci. USSR*, **28**, P. 963–971 (1986).